

# Networked Communication for Mean-Field Games with Function Approximation and Empirical Mean-Field Estimation

Patrick Benjamin Alessandro Abate

University of Oxford  
patrick.benjamin@jesus.ox.ac.uk, alessandro.abate@cs.ox.ac.uk

## Abstract

Recent works have provided algorithms by which decentralised agents, which may be connected via a communication network, can learn equilibria in Mean-Field Games from a single, non-episodic run of the empirical system. However, these algorithms are given for tabular settings: this computationally limits the size of players' observation space, meaning that the algorithms are not able to handle anything but small state spaces, nor to generalise beyond policies depending on the ego player's state to so-called 'population-dependent' policies. We address this limitation by introducing function approximation to the existing setting, drawing on the Munchausen Online Mirror Descent method that has previously been employed only in finite-horizon, episodic, centralised settings. While this permits us to include the population's mean-field distribution in the observation for each player's policy, it is arguably unrealistic to assume that decentralised agents would have access to this global information: we therefore additionally provide new algorithms that allow agents to estimate the global empirical distribution based on a local neighbourhood, and to improve this estimate via communication over a given network. Our experiments showcase how the communication network allows decentralised agents to estimate the mean-field distribution for population-dependent policies, and that exchanging policy information helps networked agents to outperform both independent and even centralised agents in function-approximation settings, by an even greater margin than in tabular settings.

## 1 Introduction

The mean-field game (MFG) framework (Lasry and Lions 2007; Huang, Malhamé, and Caines 2006) can be used to address the difficulty faced by multi-agent reinforcement learning (MARL) regarding computational scalability as the number of agents increases. It models a representative agent as interacting not with other individual agents in the population on a per-agent basis, but instead with a distribution over the other agents, known as the *mean field*. The MFG framework analyses the limiting case when the population consists of an infinite number of symmetric and anonymous agents, that is, they have identical reward and transition functions which depend on the mean-field distribution rather than on the actions of specific other players. The solution to this game is the mean-field Nash equilibrium (MFNE), which can be used as an approximation for the Nash equilibrium

(NE) in a finite-agent game, with the error in the solution reducing as the number of agents  $N$  tends to infinity (Saldi, Başar, and Raginsky 2018; Anahtarci, Kariksiz, and Saldi 2023; Yardim, Goldman, and He 2024; Toumi, Malhame, and Le Ny 2024; Hu and Zhang 2024). MFGs have thus been applied to a wide variety of real-world problems: see Laurière et al. (2022) for applications and references.

Recent works argue that classical algorithms for solving MFGs rely on assumptions and methods that are likely to be undesirable in real-world applications, emphasising that desirable qualities for practical MFG algorithms include: learning from the empirical distribution of  $N$  agents (without generation or manipulation of this distribution by the algorithm itself or an external oracle/simulator); learning from a single, continued system run that is not arbitrarily reset as in episodic learning; model-free learning; decentralisation; and fast practical convergence (Yardim et al. 2023; Benjamin and Abate 2024). While these works address these desiderata, they do so only in settings in which the state and action spaces are small enough that the Q-function can be represented by a table, limiting their approaches' scalability.

Moreover, in those works, as in many others on MFGs, agents only observe their local state as input to their Q-function (which defines their policy). This is sufficient when the solved MFG is expected to have a stationary distribution ('stationary MFGs') (Laurière et al. 2022; Xie et al. 2021; Anahtarci, Kariksiz, and Saldi 2023; uz Zaman et al. 2023; Yardim et al. 2023; Benjamin and Abate 2024). However, in reality there are numerous reasons for which agents may benefit from being able to respond to the current distribution. Recent work has thus increasingly focused on these more general settings where it is necessary for agents to have so-called 'master policies' (a.k.a. population-dependent policies) which depend on both the mean-field distribution and their local state (Cardaliaguet et al. 2015; Carmona, Delarue, and Lacker 2016; Perrin et al. 2022; Wu et al. 2024; Laurière et al. 2022; Lauriere et al. 2022; Laurière et al. 2022).

The distribution is a high-dimensional (and thus large) observation object, and also takes a continuum of values. Therefore a population-dependent Q-function cannot be represented exactly in a table and must be approximated. To address these limitations while maintaining the desiderata for real-world applications given in recent works, we introduce function approximation to the MFG setting of decentralised

agents learning from a single, non-episodic run of the empirical system, allowing this setting to handle larger state spaces and to accept the mean-field distribution as an observation input. To overcome the difficulties of training non-linear approximators in this context, we use the so-called ‘Munchausen’ trick, introduced by Vieillard, Pietquin, and Geist (2020) for single-agent RL, and extended to MFGs by Lauriere et al. (2022), and to MFGs with population-dependent policies by Wu et al. (2024).

We particularly explore this in the context of networked communication between decentralised agents (Benjamin and Abate 2024). We demonstrate that this communication brings two specific benefits over the purely independent setting (while also removing the undesirable assumption of a centralised learner, which in the real world may be unrealistic, a computational bottleneck and a vulnerable single point of failure). Firstly, when the Q-function is approximated rather than exact, some updates lead to better performing policies than others. Allowing networked agents to propagate better performing policies through the population leads to faster practical convergence than in the purely independent-learning case, and often even than in the centralised case. Secondly, we argue that in the real world it is unrealistic to assume that decentralised agents, endowed with local state observations and limited (if any) communication radius, would be able to observe the global mean-field distribution and use it as input to their Q-functions / policy. We therefore further contribute two setting-dependent algorithms by which decentralised agents can estimate the global distribution from local observations, and further improve their estimates by communication with neighbours.

We focus on ‘coordination games’, where agents can increase their individual rewards by following the same strategy as others and therefore have an incentive to communicate policies, even if the MFG setting itself is technically non-cooperative. Thus our work can be applied to real-world problems in e.g. traffic signal control, formation control in swarm robotics, and consensus and synchronisation e.g. for sensor networks. In summary, our contributions are:

- We introduce, for the first time, function approximation to MFG settings with decentralised agents. To do this:
  - We use Munchausen RL for the first time in an infinite-horizon MFG context, unlike the finite-horizon settings in Lauriere et al. (2022) and Wu et al. (2024).
  - In doing so, we also present the first use of function approximation for solving MFGs from continued, non-episodic runs of the empirical system; this is unlike Yardim et al. (2023) and Benjamin and Abate (2024), which look at tabular settings.
- Function approximation allows us to explore larger state spaces, and also settings where agents’ policies depend on the mean-field distribution as well as their local state.
- Rather than assuming that agents have access to this global knowledge, as in prior works, we present two novel algorithms that allow decentralised agents to locally estimate the empirical distribution and to improve these estimates by communication with others.

- We present numerical results showcasing these algorithms, especially the two benefits of the decentralised communication scheme, which significantly outperforms both the independent and centralised settings.

The paper is structured as follows. Preliminaries are given in Sec. 2 and our core learning and policy improvement algorithm is presented in Sec. 3. Our mean-field estimation and communication algorithms are given in Sec. 4, and experiments are presented in Sec. 5. See Appx. B for a more detailed ‘Related work’ section. Ways to extend our algorithms are discussed in the ‘Future Work’ section (Appx. C).

## 2 Preliminaries

### 2.1 Mean-field games

We use the following notation.  $N$  is the number of agents in a population, with  $\mathcal{S}$  and  $\mathcal{A}$  representing the finite state and common action spaces, respectively. The set of probability measures on a finite set  $\mathcal{X}$  is denoted  $\Delta_{\mathcal{X}}$ , and  $\mathbf{e}_x \in \Delta_{\mathcal{X}}$  for  $x \in \mathcal{X}$  is a one-hot vector with only the entry corresponding to  $x$  set to 1, and all others set to 0. For time  $t \geq 0$ ,  $\hat{\mu}_t = \frac{1}{N} \sum_{i=1}^N \sum_{s \in \mathcal{S}} \mathbb{1}_{s_t^i=s} \mathbf{e}_s \in \Delta_{\mathcal{S}}$  is a vector of length  $|\mathcal{S}|$  denoting the empirical categorical state distribution of the  $N$  agents at time  $t$ . For agent  $i \in 1 \dots N$ ,  $i$ ’s policy at time  $t$  depends on its observation  $o_t^i$ . We explore three different forms that this observation object can take:

- In the conventional setting, the observation is simply  $i$ ’s current local state  $s_t^i$ , such that  $\pi^i(a|o_t^i) = \pi^i(a|s_t^i)$ .
- When the policy is population-dependent, if we assume perfect observability of the global mean-field distribution then we have  $o_t^i = (s_t^i, \hat{\mu}_t)$ .
- It is unrealistic to assume that decentralised agents with a possibly limited communication radius can observe the global mean-field distribution, so we allow agents to form a local estimate  $\tilde{\mu}_t^i$  which can be improved by communication with neighbours. Here we have  $o_t^i = (s_t^i, \tilde{\mu}_t^i)$ .

In the following definitions we focus on the population-dependent case when  $o_t^i = (s_t^i, \hat{\mu}_t)$ , and clarify afterwards the connection to the other observation cases. Thus the set of policies is  $\Pi = \{\pi : \mathcal{S} \times \Delta_{\mathcal{S}} \rightarrow \Delta_{\mathcal{A}}\}$ , and the set of Q-functions is denoted  $\mathcal{Q} = \{q : \mathcal{S} \times \Delta_{\mathcal{S}} \times \mathcal{A} \rightarrow \mathbb{R}\}$ .

#### Definition 1 (*N*-player symmetric anonymous games)

An *N*-player stochastic game with symmetric, anonymous agents is given by the tuple  $\langle N, \mathcal{S}, \mathcal{A}, P, R, \gamma \rangle$ , where  $\mathcal{A}$  is the action space, identical for each agent;  $\mathcal{S}$  is the identical state space of each agent, such that their initial states are  $\{s_0^i\}_{i=1}^N \in \mathcal{S}^N$  and their policies are  $\{\pi^i\}_{i=1}^N \in \Pi^N$ .  $P : \mathcal{S} \times \mathcal{A} \times \Delta_{\mathcal{S}} \rightarrow \Delta_{\mathcal{S}}$  is the transition function and  $R : \mathcal{S} \times \mathcal{A} \times \Delta_{\mathcal{S}} \rightarrow [0,1]$  is the reward function, which map each agent’s local state and action and the population’s empirical distribution to transition probabilities and bounded rewards, respectively, i.e.  $\forall i = 1, \dots, N$ :

$$s_{t+1}^i \sim P(\cdot | s_t^i, a_t^i, \hat{\mu}_t), \quad r_t^i = R(s_t^i, a_t^i, \hat{\mu}_t).$$

At the limit as  $N \rightarrow \infty$ , the infinite population of agents can be characterised as a limit distribution  $\mu \in \Delta_{\mathcal{S}}$ ; the

infinite-agent game is termed an MFG. The so-called ‘mean-field flow’  $\boldsymbol{\mu}$  is given by the infinite sequence of mean-field distributions s.t.  $\boldsymbol{\mu} = (\mu_t)_{t \geq 0}$ .

**Definition 2 (Induced mean-field flow)** We denote by  $I(\pi)$  the mean-field flow  $\boldsymbol{\mu}$  induced when all the agents follow  $\pi$ , where this is generated from  $\pi$  as follows:

$$\mu_{t+1}(s') = \sum_{s,a} \mu_t(s) \pi(a|s, \mu_t) P(s'|s, a, \mu_t).$$

When the mean-field flow is stationary such that the distribution is the same for all  $t$ , i.e.  $\mu_t = \mu_{t+1} \forall t \geq 0$ , the policy  $\pi^i(a|s_t^i, \mu_t)$  need not depend on the distribution, such that  $\pi^i(a|s_t^i, \mu_t) = \pi^i(a|s_t^i)$ , i.e. we recover the classical population-independent policy. However, for such a population-independent policy the initial distribution  $\mu_0$  must be known and fixed in advance, whereas otherwise it need not be. We also give the following definitions.

**Definition 3 (Mean-field discounted return)** In a MFG where all agents follow policy  $\pi$  giving a mean-field flow  $\boldsymbol{\mu} = (\mu_t)_{t \geq 0}$ , the expected discounted return of the representative agent is given by

$$V(\pi, \boldsymbol{\mu}) = \mathbb{E} \left[ \sum_{t=0}^{\infty} \gamma^t (R(s_t, a_t, \mu_t)) \middle| \begin{array}{l} s_0 \sim \mu_0 \\ a_t \sim \pi(\cdot | s_t, \mu_t) \\ s_{t+1} \sim P(\cdot | s_t, a_t, \mu_t) \end{array} \right].$$

**Definition 4 (Best-response (BR) policy)** A policy  $\pi^*$  is a best response (BR) against the mean-field flow  $\boldsymbol{\mu}$  if it maximises the discounted return  $V(\cdot, \boldsymbol{\mu})$ ; the set of these policies is denoted  $BR(\boldsymbol{\mu})$ , i.e.

$$\pi^* \in BR(\boldsymbol{\mu}) := \arg \max_{\pi} V(\pi, \boldsymbol{\mu}).$$

**Definition 5 (Mean-field Nash equilibrium (MFNE))** A pair  $(\pi^*, \boldsymbol{\mu}^*)$  is a mean-field Nash equilibrium (MFNE) if the following two conditions hold:

- $\pi^*$  is a best response to  $\boldsymbol{\mu}^*$ , i.e.  $\pi^* \in BR(\boldsymbol{\mu}^*)$ ;
- $\boldsymbol{\mu}^*$  is induced by  $\pi^*$ , i.e.  $\boldsymbol{\mu}^* = I(\pi^*)$ .

$\pi^*$  is thus a fixed point of the map  $BR \circ I$ , i.e.  $\pi^* \in BR(I(\pi^*))$ . If a population-dependent policy is a MFNE policy for any initial distribution  $\mu_0$ , it is a ‘master policy’.

Previous works have shown that, in tabular settings, it is possible for a finite population of decentralised agents (each of which is permitted to have a distinct population-independent policy  $\pi^i$ ) to learn the MFNE using only the empirical distribution  $\hat{\mu}_t$ , rather than the exactly calculated mean-field flow (Yardim et al. 2023; Benjamin and Abate 2024). This MFNE is in turn an approximate NE for the original finite-agent game. In this work we provide algorithms to perform this in non-tabular and population-dependent settings, and demonstrate them empirically.

## 2.2 (Munchausen) Online Mirror Descent

Instead of performing the computationally expensive process of finding a BR at each iteration, we can use a form of policy iteration for MFGs called Online Mirror Descent (OMD). This involves beginning with an initial policy  $\pi_0$ , and then at each iteration  $k$ , evaluating the current policy

$\pi_k$  with respect to its induced mean-field flow  $\boldsymbol{\mu} = I(\pi_k)$  to compute its Q-function  $Q_{k+1}$ . To stabilise the learning process, we then use a weighted sum over this and past Q-functions, and set  $\pi_{k+1}$  to be the softmax over this weighted sum, i.e.  $\pi_{k+1}(\cdot|s, \boldsymbol{\mu}) = \text{softmax} \left( \frac{1}{\tau_q} \sum_{\kappa=0}^k Q_{\kappa}(s, \boldsymbol{\mu}, \cdot) \right)$ .  $\tau_q$  is a temperature parameter that scales the entropy in Munchausen RL (Vieillard, Pietquin, and Geist 2020); note that this is a different temperature to the one agents use when selecting which communicated parameters to adopt, denoted  $\tau_k^{comm}$  and discussed in Sec. 3.2.

If the Q-function is approximated non-linearly using neural networks, it is difficult to compute this weighted sum. The so-called ‘Munchausen trick’ addresses this by computing a single Q-function that mimics the weighted sum using implicit regularisation based on the Kullback-Leibler (KL) divergence between  $\pi_k$  and  $\pi_{k+1}$  (Vieillard, Pietquin, and Geist 2020). Using this reparametrisation gives Munchausen OMD (MOMD), detailed further in Sec. 3.1 (Lauriere et al. 2022; Wu et al. 2024). MOMD does not bias the MFNE, and has the same convergence guarantees as OMD (Hadikhlanloo 2017; Pérolat et al. 2022a; Wu et al. 2024).

## 2.3 Networks

We conceive of the finite population as exhibiting two time-varying networks. The basic definition of such a network is:

**Definition 6 (Time-varying network)** The time-varying network  $\{\mathcal{G}_t\}_{t \geq 0}$  is given by  $\mathcal{G}_t = (\mathcal{N}, \mathcal{E}_t)$ , where  $\mathcal{N}$  is the set of vertices each representing an agent  $i = 1, \dots, N$ , and the edge set  $\mathcal{E}_t \subseteq \{(i,j) : i,j \in \mathcal{N}\}$  is the set of undirected links present at time  $t$ .

One of these networks  $\mathcal{G}_t^{comm}$  defines which agents are able to communicate information to each other at time  $t$ . The second network  $\mathcal{G}_t^{obs}$  is a graph defining which agents are able to observe each other’s states, which we use in general settings for estimating the mean-field distribution from local information. The structure of the two networks may be identical (e.g. if embodied agents can both observe the position (state) of, and exchange information with, other agents within a certain physical distance from themselves), or different (e.g. if agents can observe the positions of nearby agents, but only exchange information with agents by which they are connected via a telephone line, which may connect agents over long distances).

We also define an alternative version of the observation graph that is useful in a specific subclass of environments, which can most intuitively be thought of as those where agents’ states are positions in physical space. When this is the case, we usually think of agents’ ability to observe each other as depending more abstractly on whether states are visible to each other. We define this visibility graph as follows:

**Definition 7 (Time-varying state-visibility graph)** The time-varying state visibility graph  $\{\mathcal{G}_t^{vis}\}_{t \geq 0}$  is given by  $\mathcal{G}_t^{vis} = (\mathcal{S}', \mathcal{E}_t^{vis})$ , where  $\mathcal{S}'$  is the set of vertices representing the environment states  $\mathcal{S}$ , and the edge set  $\mathcal{E}_t^{vis} \subseteq \{(m,n) : m,n \in \mathcal{S}'\}$  is the set of undirected links present at time  $t$ , indicating which states are visible to each other.

We view an agent in  $s$  as able to obtain a count of the number of agents in  $s'$  if  $s'$  is visible to  $s$ . The benefit of this graph  $\mathcal{G}_t^{vis}$  over  $\mathcal{G}_t^{obs}$  is that there is mutual exclusivity: either an agent in state  $s$  is able to obtain a total count of all of the agents in state  $s'$  (if  $s'$  is visible to  $s$ ), or it cannot obtain information about any agent in state  $s'$  (if those states are not visible to each other). Additionally, this graph permits an agent in state  $s$  to observe that there are *no* agents in state  $s'$  as long as  $s'$  is visible to  $s$ . These benefits are not available if the observability graph is defined strictly between agents as in  $\mathcal{G}_t^{obs}$ , such that using  $\mathcal{G}_t^{vis}$  facilitates more efficient estimation of the global mean-field distribution from local information in settings where  $\mathcal{G}_t^{vis}$  is applicable (see Sec. 4).

### 3 Learning and policy improvement

#### 3.1 Q-network and update

Lines 1-14 of our novel Alg. 1 contain the core Q-function/policy update method. Agent  $i$  maintains a neural network parametrised by  $\theta_k^i$  to approximate its Q-function:  $\tilde{Q}_{\theta_k^i}(o, \cdot)$ . The agent's policy is given by  $\pi_{\theta_k^i}(a|o) = \text{softmax}\left(\frac{1}{\tau_q} \tilde{Q}_{\theta_k^i}(o, \cdot)\right)(a)$ . When appropriate, we denote the policy  $\pi_k^i(a|o)$  for simplicity. Each agent maintains a buffer (with size  $M$ ) of collected transitions of the form  $(o_t^i, a_t^i, r_t^i, o_{t+1}^i)$ . At each iteration  $k$ , they empty their buffer (Line 3) before collecting  $M$  new transitions (Lines 4-7); each decentralised agent  $i$  then trains its Q-network  $\tilde{Q}_{\theta_k^i}$  via  $L$  training updates as follows (Lines 8-12). For training purposes,  $i$  also maintains a target network  $\tilde{Q}_{\theta_{k,l}^{i'}}$  with the same architecture but parameters  $\theta_{k,l}^{i'}$  copied from  $\theta_{k,l}^i$  less regularly than  $\theta_{k,l}^i$  themselves are updated, i.e. only every  $\nu$  learning iterations (Line 11). At each iteration  $l$ , the agent samples a random batch  $B_{k,l}^i$  of  $|B|$  transitions from its buffer (Line 9). It then trains its neural network using stochastic gradient descent to minimise the following empirical loss (Line 10):

**Definition 8 (Empirical loss for Q-network)** *The empirical loss is given by*

$$\hat{L}(\theta, \theta') = \frac{1}{|B|} \sum_{\text{transition} \in B_{k,l}^i} \left| \tilde{Q}_{\theta_{k,l}^{i'}}(o_t, a_t) - T \right|^2,$$

where the target  $T$  is

$$T = r_t + [\tau_q \ln \pi_{\theta_{k,l}^{i'}}(a_t|o_t)]_{cl}^0 + \gamma \sum_{a \in \mathcal{A}} \pi_{\theta_{k,l}^{i'}}(a|o_{t+1}) \left( \tilde{Q}_{\theta_{k,l}^{i'}}(o_{t+1}, a) - \tau_q \ln \pi_{\theta_{k,l}^{i'}}(a|o_{t+1}) \right).$$

For  $cl < 0$ ,  $[\cdot]_{cl}^0$  is a clipping function used in Munchausen RL to prevent numerical issues if the policy is too close to deterministic, as the log-policy term is otherwise unbounded (Vieillard, Pietquin, and Geist 2020; Wu et al. 2024).

#### 3.2 Communication and adoption of parameters

We use the communication network  $\mathcal{G}_t^{comm}$  to share two types of information at different points in Alg 1. One is used

---

Algorithm 1: Networked learning with non-linear function approximation

---

**Require:** loop parameters  $K, M, L, E, C_p$ , learning parameters  $\gamma, \tau_q, |B|, cl, \nu, \{\tau_k^{comm}\}_{k \in \{0, \dots, K-1\}}$   
**Require:** initial states  $\{s_0^i\}_i, i = 1, \dots, N; t \leftarrow 0$   
1:  $\forall i$  : Randomly initialise parameters  $\theta_0^i$  of Q-networks  $\tilde{Q}_{\theta_0^i}(o_t^i, \cdot)$ , and set  $\pi_0^i(a|o) = \text{softmax}\left(\frac{1}{\tau_q} \tilde{Q}_{\theta_0^i}(o, \cdot)\right)(a)$   
2: **for**  $k = 0, \dots, K - 1$  **do**  
3:  $\forall i$ : Empty  $i$ 's buffer  
4: **for**  $m = 0, \dots, M - 1$  **do**  
5: Take step  $\forall i$  :  $a_t^i \sim \pi_k^i(\cdot|o_t^i), r_t^i = R(s_t^i, a_t^i, \hat{\mu}_t), s_{t+1}^i \sim P(\cdot|s_t^i, a_t^i, \hat{\mu}_t); t \leftarrow t + 1$   
6:  $\forall i$ : Add  $\zeta_t^i$  to  $i$ 's buffer  
7: **end for**  
8: **for**  $l = 0, \dots, L - 1$  **do**  
9:  $\forall i$  : Sample batch  $B_{k,l}^i$  from  $i$ 's buffer  
10: Update  $\theta$  to minimise  $\hat{L}(\theta, \theta')$  as in Def. 8  
11: If  $l \bmod \nu = 0$ , set  $\theta' \leftarrow \theta$   
12: **end for**  
13:  $\tilde{Q}_{\theta_{k+1}^i}(o, \cdot) \leftarrow \tilde{Q}_{\theta_{k,L}^i}(o, \cdot)$   
14:  $\forall i$  : Set  $\pi_{k+1}^i(a|o) = \text{softmax}\left(\frac{1}{\tau_q} \tilde{Q}_{\theta_{k+1}^i}(o, \cdot)\right)(a)$   
15:  $\forall i$  :  $\sigma_{k+1}^i = 0$   
16: **for**  $e = 0, \dots, E - 1$  evaluation steps **do**  
17: Take step  $\forall i$  :  $a_t^i \sim \pi_k^i(\cdot|o_t^i), r_t^i = R(s_t^i, a_t^i, \hat{\mu}_t), s_{t+1}^i \sim P(\cdot|s_t^i, a_t^i, \hat{\mu}_t); t \leftarrow t + 1$   
18:  $\forall i$  :  $\sigma_{k+1}^i = \sigma_{k+1}^i + \gamma^e (r_t^i + h(\pi_{k+1}^i(s_t^i)))$   
19:  $t \leftarrow t + 1$   
20: **end for**  
21: **for**  $C_p$  rounds **do**  
22:  $\forall i$  : Broadcast  $\sigma_{k+1}^i, \pi_{k+1}^i$   
23:  $\forall i$  :  $J_t^i \leftarrow \{j \in \mathcal{N} : (i, j) \in \mathcal{E}_t\}$   
24:  $\forall i$  : Select adopted $^i \sim \text{Pr}(\text{adopted}^i = j) = \frac{\exp(\sigma_{k+1}^j / \tau_k^{comm})}{\sum_{x \in J_t^i} \exp(\sigma_{k+1}^x / \tau_k^{comm})} \forall j \in J_t^i$   
25:  $\forall i$  :  $\sigma_{k+1}^i \leftarrow \sigma_{k+1}^{\text{adopted}^i}, \pi_{k+1}^i \leftarrow \pi_{k+1}^{\text{adopted}^i}$   
26: Take step  $\forall i$  :  $a_t^i \sim \pi_k^i(\cdot|o_t^i), r_t^i = R(s_t^i, a_t^i, \hat{\mu}_t), s_{t+1}^i \sim P(\cdot|s_t^i, a_t^i, \hat{\mu}_t); t \leftarrow t + 1$   
27: **end for**  
28: **end for**  
29: **return** policies  $\{\pi_K^i\}_i, i = 1, \dots, N$

---

to improve local estimates of the mean-field distribution (see Sec. 4). The other, described here, is used to privilege the spread of better performing policy updates through the population, allowing faster convergence in this networked case than in the independent and even centralised cases.

We extend the work in Benjamin and Abate (2024) to the function-approximation case, where in our work agents broadcast the parameters of the Q-network that defines their policy, rather than the Q-function table. At each iteration  $k$ , after independently updating their Q-network and policy (Lines 3-14), agents approximately evaluate their new policies by collecting rewards for  $E$  steps, and assign the es-

---

Algorithm 2: Mean-field estimation and communication algorithm in general settings

---

**Require:** Time-dependent observation graph  $\mathcal{G}_t^{obs}$ , time-dependent communication graph  $\mathcal{G}_t^{comm}$ , states  $\{s_t^i\}_{i=1}^N$ , number of communication rounds  $C_e$

- 1:  $\forall i, s$  : Initialise count vector  $\hat{v}_t^i[s]$  with  $\emptyset$
- 2:  $\forall i$  :  $\hat{v}_t^i[s_t^j] \leftarrow \{ID^j\}_{j \in \mathcal{N} : (i,j) \in \mathcal{E}_t^{obs}}$
- 3: **for**  $c_e$  in  $1, \dots, C_e$  **do**
- 4:  $\forall i$  : Broadcast  $\hat{v}_{t,c_e}^i$
- 5:  $\forall i$  :  $J_t^i \leftarrow \{j \in \mathcal{N} : (i,j) \in \mathcal{E}_t^{comm}\}$
- 6:  $\forall i, s$  :  $\hat{v}_{t,(c_e+1)}^i[s] \leftarrow \hat{v}_{t,c_e}^i[s] \cup \{\hat{v}_{t,c_e}^j[s]\}_{j \in J_t^i}$
- 7: **end for**
- 8:  $\forall i$  :  $counted\_agents_t^i \leftarrow \sum_{s \in \mathcal{S} : \hat{v}_t^i[s] \neq \emptyset} |\hat{v}_t^i[s]|$
- 9:  $\forall i$  :  $uncounted\_agents_t^i \leftarrow N - counted\_agents_t^i$
- 10:  $\forall i, s$  :  $\tilde{\mu}_t^i[s] \leftarrow \frac{uncounted\_agents_t^i}{N \times |\mathcal{S}|}$
- 11:  $\forall i, s$  where  $\hat{v}_t^i[s]$  is not  $\emptyset$  :  $\tilde{\mu}_t^i[s] \leftarrow \tilde{\mu}_t^i[s] + \frac{|\hat{v}_t^i[s]|}{N}$
- 12: **return** mean-field estimates  $\forall i \tilde{\mu}_t^i$

---

timated value to  $\sigma_{k+1}^i$  (Lines 15-20). They then broadcast their Q-network parameters along with  $\sigma_{k+1}^i$  (Line 22). Receiving these from their neighbours on the communication network, agents select which set of parameters to adopt by taking a softmax over their own and the received estimate values  $\sigma_{k+1}^j$  (Lines 23-25). They repeat this broadcast and adoption process for  $C_p$  rounds, which is distinct from the  $C_e$  communication rounds discussed in Sec. 4. By this process, decentralised agents can adopt policy parameters that are estimated to be better performing than their own, bringing the benefits to convergence speed discussed in Sec. 5.1.

#### 4 Mean-field estimation and communication

We first describe the most general version of our algorithm for decentralised estimation of the empirical categorical mean-field distribution, assuming the more general setting where  $\mathcal{G}_t^{obs}$  applies (see discussion in Sec. 2.3). We subsequently detail how the algorithm can be made more efficient in environments where the more abstract visibility graph  $\mathcal{G}_t^{vis}$  applies, as in our experimental settings. In both cases, the algorithm runs to generate the observation object when a step is taken in the main Alg. 1, i.e. to produce  $o_t^i = (s_t^i, \tilde{\mu}_t^i)$  for the steps  $a_t^i \sim \pi_k^i(\cdot | o_t^i)$  in Lines 5, 17 and 26. Both versions of the algorithm are subject to implicit assumptions, which we highlight and discuss methods for addressing in our ‘Future Work’ section in Appx. C.

**Algorithm for the general setting** The method for the general setting functions is given in Alg 2. In this setting, we assume that each agent is associated with a unique ID to avoid the same agents being counted multiple times. Each agent maintains a ‘count’ vector  $\hat{v}_t^i$  of length  $|\mathcal{S}|$  i.e. it is the same shape as the vector denoting the true empirical categorical distribution of agents. Each state position in the vector can hold a list of IDs. Before any actions are taken at each time step  $t$ , each agent’s count vector  $\hat{v}_t^i$  is initialised

---

Algorithm 3: Mean-field estimation and communication algorithm for environments with  $\mathcal{G}_t^{vis}$

---

**Require:** Time-dependent visibility graph  $\mathcal{G}_t^{vis}$ , time-dependent communication graph  $\mathcal{G}_t^{comm}$ , states  $\{s_t^i\}_{i=1}^N$ , number of communication rounds  $C_e$

- 1:  $\forall i, s$  : Initialise count vector  $\hat{v}_t^i[s]$  with  $\emptyset$
- 2:  $\forall i$  and  $\forall s' \in \mathcal{S}' : (s_t^i, s') \in \mathcal{E}_t^{vis} : \hat{v}_t^i[s'] \leftarrow \sum_{j \in \{1, \dots, N : s_t^j = s'\}} 1$
- 3: **for**  $c_e$  in  $1, \dots, C_e$  **do**
- 4:  $\forall i$  : Broadcast  $\hat{v}_{t,c_e}^i$
- 5:  $\forall i$  :  $J_t^i = i \cup \{j \in \mathcal{N} : (i,j) \in \mathcal{E}_t^{comm}\}$
- 6:  $\forall i, s$  and  $\forall j \in J_t^i : \hat{v}_{t,(c_e+1)}^i[s] \leftarrow \hat{v}_{t,c_e}^i[s]$  if  $\hat{v}_{t,c_e}^j[s] \neq \emptyset$
- 7: **end for**
- 8:  $\forall i$  :  $counted\_agents_t^i \leftarrow \sum_{s \in \mathcal{S} : \hat{v}_t^i[s] \neq \emptyset} \hat{v}_t^i[s]$
- 9:  $\forall i$  :  $uncounted\_agents_t^i \leftarrow N - counted\_agents_t^i$
- 10:  $\forall i$  :  $unseen\_states_t^i \leftarrow \sum_{s \in \mathcal{S} : \hat{v}_t^i[s] = \emptyset} 1$
- 11:  $\forall i, s$  where  $\hat{v}_t^i[s]$  is not  $\emptyset$  :  $\tilde{\mu}_t^i[s] \leftarrow \frac{\hat{v}_t^i[s]}{N}$
- 12:  $\forall i, s$  where  $\hat{v}_t^i[s]$  is  $\emptyset$  :  $\tilde{\mu}_t^i[s] \leftarrow \frac{uncounted\_agents_t^i}{N \times unobserved\_states_t^i}$
- 13: **return** mean-field estimates  $\forall i \tilde{\mu}_t^i$

---

as full of  $\emptyset$  (‘no count’) markers for each state. Then, for each agent  $j$  with which agent  $i$  is connected via the observation graph,  $i$  places  $j$ ’s unique ID in its count vector in the correct state position. Next, for  $C_e \geq 0$  communication rounds, agents exchange their local counts with neighbours on the communication network, and merge these counts with their own count vector, filtering out the unique IDs of those that have already been counted. If  $C_e = 0$  then the local count will remain purely independent. By exchanging these partially filled vectors, agents are able to improve their local counts by adding the states of agents that they have not been able to observe directly themselves.

After the  $C_e$  communication rounds, each state position  $\hat{v}_t^i[s]$  either still maintains the  $\emptyset$  marker if no agents have been counted in this state, or it contains  $x_s > 0$  unique IDs. The local mean-field estimate  $\tilde{\mu}_t^i$  is then obtained from  $\hat{v}_t^i$  as follows. All states that have a count  $x_s$  have this count converted into the categorical probability  $x_s/N$  (we assume that agents know the total number of agents in the finite population, even if they cannot observe them all at each  $t$ ). The total number of agents counted in  $\hat{v}_t^i$  is given by  $counted\_agents = \sum_{s \in \mathcal{S}} x_s$ , and the agents that have not been observed are  $uncounted\_agents = N - counted\_agents$ . In this general setting, the unobserved agents are assumed to be uniformly distributed across all the states, so  $uncounted\_agents/(N \times |\mathcal{S}|)$  is added to all the values in  $\tilde{\mu}_t^i$ , replacing the  $\emptyset$  marker for states for which no agents have been observed.

**Algorithm for visibility-based environments** We now describe the differences in our estimation algorithm (Alg. 3) for the subclass of environments where  $\mathcal{G}_t^{vis}$  applies in place of  $\mathcal{G}_t^{obs}$ , i.e. the mutual observability of agents depends in

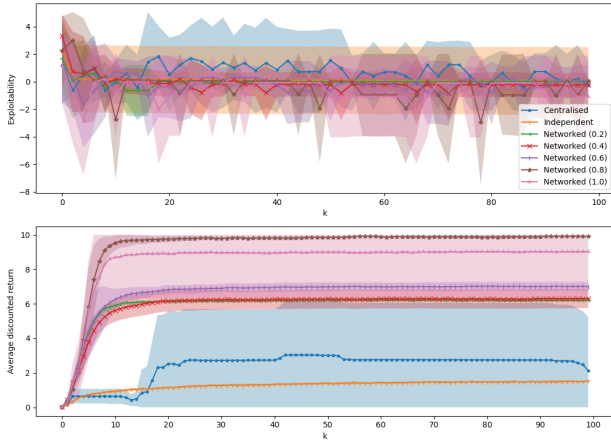


Figure 1: ‘Target agreement’ task, population-independent policies, 50x50 grid.

turn on the mutual visibility of states. Recall the benefit of  $\mathcal{G}_t^{vis}$  over  $\mathcal{G}_t^{obs}$  is that the former allows an agent in state  $s$  to obtain a correct, complete count  $x_{s'} \geq 0$  of all the agents in state  $s'$ , for any state  $s'$  that is visible to  $s$  (note the count may be zero). Unique IDs are thus not required as there is no risk of counting the same agent twice when receiving communicated counts: either *all* agents in  $s'$  have been counted, or no count has yet been obtained for  $s'$ . This simplifies the algorithm and helps preserve agent anonymity and privacy.

Secondly, uncounted agents cannot be in states for which a count has already been obtained, since the count is complete and correct, even if the count is  $x_{s'} = 0$ . Therefore after the  $C_e$  communication rounds, the uncounted agents  $uncounted/N$  need be uniformly distributed only across the positions in the vector that still have the  $\emptyset$  marker, and not across all states as in the general setting. This makes the estimation more accurate in this special setting.

## 5 Experiments

We provide two sets of experiments. The first set showcases that our function-approximation algorithm (Alg. 1) can scale to large state spaces for population-independent policies, and that in such settings networked, communicating agents can outperform purely-independent and even centralised agents, and do so by an even greater margin than in the tabular settings from Benjamin and Abate (2024). The second set demonstrates that Alg. 1 can handle population-dependent policies, as well as the ability of Alg. 3 to practically estimate the mean-field distribution locally.

For the types of game used in our demonstrations we follow the gold standard in prior works on MFGs, namely grid-world environments where agents can move in the four cardinal directions or remain in place (uz Zaman et al. 2023; Lauriere et al. 2022; Algumaei et al. 2023; Laurière 2021; Cui, Fabian, and Koeppl 2023; Lauriere et al. 2022; Benjamin and Abate 2024; Wu et al. 2024). We present results from four *coordination* tasks defined by the reward/transition functions of the agents - see Appx. A.1 for a

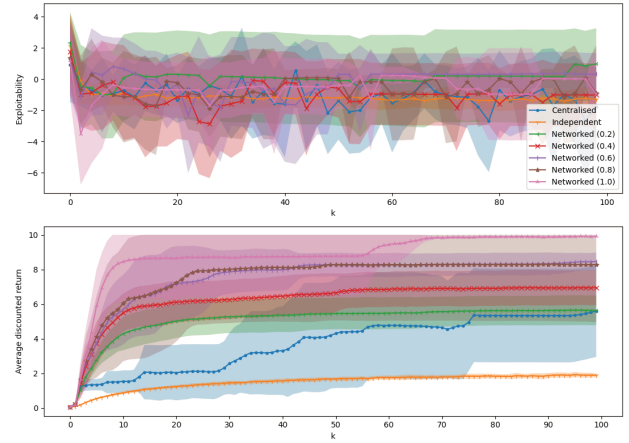


Figure 2: ‘Cluster’ task, population-independent policies, 100x100 grid.

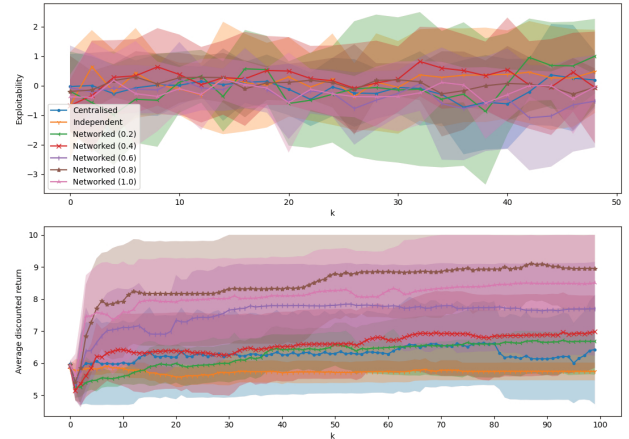


Figure 3: ‘Push object’ task, population-dependent policies with estimated mean-field distribution, 10x10 grid.

full technical description. The first two tasks are those used with population-independent policies in Benjamin and Abate (2024), though while they show results for an 8x8 and a ‘larger’ 16x16 grid, our results for these tasks are for 100x100 and 50x50 grids:

- **Cluster.** Agents are rewarded for gathering together. The agents are given no indication where they should cluster, agreeing this themselves over time.
- **Target agreement.** Agents are rewarded for visiting any of a given number of targets, but their reward is proportional to the number of other agents co-located at the target. Agents must thus coordinate on which single target they will all meet at to maximise their individual rewards.

We also showcase the ability of our algorithm to handle two more complex tasks, using population-dependent policies and estimated mean-field observations:

- **Evade shark in shoal.** At each  $t$ , a ‘shark’ in the environment takes a step towards the grid point containing the

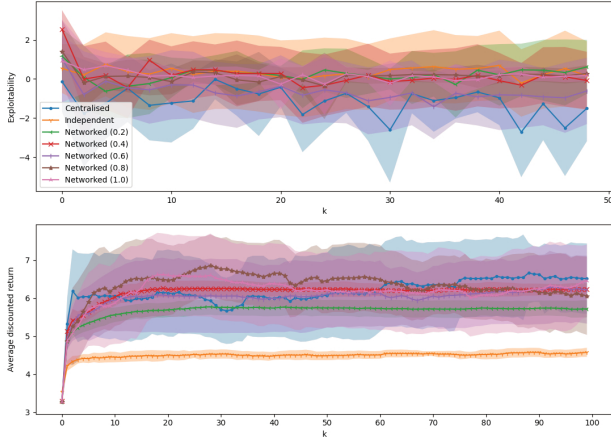


Figure 4: ‘Evade’ task, population-dependent policies with estimated mean-field distribution, 10x10 grid.

most agents according to the empirical mean-field distribution. The shark’s position forms part of agents’ local states in addition to their own position. Agents are rewarded more for being further from the shark, and also for clustering with other agents. As well as featuring a non-stationary distribution, we add ‘common noise’ to the environment, with the shark taking a random step with probability 0.01. Such noise that affects the local states of all agents in the same way, making the evolution of the distribution stochastic, makes population-independent policies sub-optimal (Laurière et al. 2022).

- **Push object to edge.** Agents are rewarded for how close they are to an ‘object’ in the environment, and for how close this object is to the edge of the grid. The object’s position forms part of agents’ local states in addition to their own position. The object moves in a direction with a probability proportional to the number of agents on its opposite side, i.e. agents must coordinate on which side of the object from which to ‘push’ it, to ensure it moves toward the edge of the grid.

In these spatial environments, both the communication network  $\mathcal{G}_t^{comm}$  and the visibility graph  $\mathcal{G}_t^{vis}$  are determined by the physical distance from agent  $i$ ; we show plots for various radii, expressed as fractions of the maximum possible distance (the diagonal length of the grid). To demonstrate the benefits of the networked architecture by comparison, we also plot the results of modified versions of our algorithm for centralised and independent learners. In the centralised setting, the Q-network updates of agent  $i = 1$  are automatically pushed to all other agents, and the true global mean-field distribution is always used in place of the local estimate i.e.  $\hat{\mu}_t^i = \hat{\mu}_t$ . In the independent case, there are no links in  $\mathcal{G}_t^{comm}$  or  $\mathcal{G}_t^{vis}$ , i.e.  $\mathcal{E}_t^{comm} = \mathcal{E}_t^{vis} = \emptyset$ . Hyperparameters are discussed in Appx. A.3.

## 5.1 Results

We evaluate our experiments via two metrics. *Exploitability* is the most common metric in works on MFGs, and is a

measure of proximity to the MFNE. It quantifies how much a best-responding agent can benefit by deviating from the set of policies that generate the current mean-field distribution, with a decreasing exploitability meaning the population is closer to the MFNE. However, there are several issues with this metric in our setting, such that it may give limited or noisy information (see Appx. A.2 for a full discussion). We thus also give a second metric, as in Benjamin and Abate (2024): the population’s *average discounted return*. This allows us to compare how much agents are learning policies that increase their returns, even when the exploitability metric gives us limited ability to distinguish between the desirability of the MFNEs to which populations are converging.

### Population-independent policies in large state-spaces

Figs. 1 and 2 illustrate that introducing function approximation to algorithms in this setting allows them to converge within a practical number of iterations ( $k \ll 100$ ), even for large state spaces (100x100 grids). By contrast, the tabular algorithms in Benjamin and Abate (2024) appear only just to converge by  $k = 200$  for the same tasks for the *larger* of their two grids, which is only 16x16.

In Fig. 1 the networked agents generally have lower exploitability than both centralised and independent agents, while in Fig. 2 the networked agents’ exploitability is similar to that of the other cases. However, the networked agents significantly outperform the other architectures in terms of average return on both tasks, indicating that the communication scheme helps agents to find substantially ‘preferable’ equilibria. Moreover, the margin by which the networked agents can outperform the centralised agents is much greater than in Benjamin and Abate (2024), showing that the benefits of the communication scheme are even greater in non-tabular settings. See Appx. A for further experiments with these large state spaces.

### Population-dependent policies in complex environments

Figs. 3 and 4, where agents estimate the mean-field distribution via Alg. 3, differ minimally from Figs. 5 and 6 in Appx. A, where agents directly receive the global mean-field distribution. This shows that our estimation algorithm allows agents to appropriately estimate the distribution, even with only one round of communication for agents to help each other improve their local counts. Only in the ‘push object’ task in Fig. 3, and there only with the smaller broadcast radii, do agents slightly underperform the returns of agents in the global observability case in Fig. 5, as is reasonable.

For the reasons given in Appx. A.2, the exploitability metric gives limited information in the ‘push object’ task in Fig. 3. In the ‘evade’ task in Fig. 4, exploitability suggests that centralised learners outperform the other cases. However, all of the networked cases significantly outperform the independent learners in terms of the average return to which they converge in both tasks. In the ‘push object’ task networked learners also significantly outperform centralised learners in all but the case with the smallest broadcast communication radius, while in the ‘evade’ task all networked cases perform similarly to the centralised case. Recall though that in the real world a centralised architecture is a strong assumption, a computational bottleneck and single point of failure.

## References

- Algumaei, T.; Solozabal, R.; Alami, R.; Hacid, H.; Debbah, M.; and Takac, M. 2023. Regularization of the policy updates for stabilizing Mean Field Games. arXiv:2304.01547.
- Anaharci, B.; Kariksiz, C. D.; and Saldi, N. 2023. Q-learning in regularized mean-field games. *Dynamic Games and Applications*, 13(1): 89–117.
- Benjamin, P.; and Abate, A. 2024. Networked Communication for Decentralised Agents in Mean-Field Games. arXiv:2306.02766.
- Cardaliaguet, P.; Delarue, F.; Lasry, J.-M.; and Lions, P.-L. 2015. The master equation and the convergence problem in mean field games. arXiv:1509.02505.
- Carmona, R.; Delarue, F.; and Lacker, D. 2016. Mean Field Games with Common Noise. *The Annals of Probability*, 44(6): 3740–3803.
- Cui, K.; Fabian, C.; and Koepl, H. 2023. Multi-Agent Reinforcement Learning via Mean Field Control: Common Noise, Major Agents and Approximation Properties. arXiv:2303.10665.
- Cui, K.; and Koepl, H. 2021. Approximately Solving Mean Field Games via Entropy-Regularized Deep Reinforcement Learning.
- Guo, X.; Hu, A.; Xu, R.; and Zhang, J. 2020. A General Framework for Learning Mean-Field Games.
- Hadikhannloo, S. 2017. Learning in anonymous nonatomic games with applications to first-order mean field games. arXiv:1704.00378.
- Hu, A.; and Zhang, J. 2024. MF-OML: Online Mean-Field Reinforcement Learning with Occupation Measures for Large Population Games. arXiv:2405.00282.
- Huang, M.; Malhamé, R. P.; and Caines, P. E. 2006. Large population stochastic dynamic games: closed-loop McKean-Vlasov systems and the Nash certainty equivalence principle. *Communications in Information & Systems*, 6(3): 221 – 252.
- Lasry, J.-M.; and Lions, P.-L. 2007. Mean Field Games. *Japanese Journal of Mathematics*, 2(1): 229–260.
- Lauriere, M.; Perrin, S.; Girgin, S.; Muller, P.; Jain, A.; Cabannes, T.; Piliouras, G.; Perolat, J.; Elie, R.; Pietquin, O.; and Geist, M. 2022. Scalable Deep Reinforcement Learning Algorithms for Mean Field Games. In Chaudhuri, K.; Jegelka, S.; Song, L.; Szepesvari, C.; Niu, G.; and Sabato, S., eds., *Proceedings of the 39th International Conference on Machine Learning*, volume 162 of *Proceedings of Machine Learning Research*, 12078–12095. PMLR.
- Laurière, M. 2021. Numerical Methods for Mean Field Games and Mean Field Type Control. arXiv:2106.06231.
- Laurière, M.; Perrin, S.; Geist, M.; and Pietquin, O. 2022. Learning Mean Field Games: A Survey.
- Pérolat, J.; Perrin, S.; Elie, R.; Laurière, M.; Piliouras, G.; Geist, M.; Tuyls, K.; and Pietquin, O. 2022a. Scaling Mean Field Games by Online Mirror Descent. In *Proceedings of the 21st International Conference on Autonomous Agents and Multiagent Systems*, AAMAS '22, 1028–1037. Richland, SC: International Foundation for Autonomous Agents and Multiagent Systems. ISBN 9781450392136.
- Pérolat, J.; Perrin, S.; Elie, R.; Laurière, M.; Piliouras, G.; Geist, M.; Tuyls, K.; and Pietquin, O. 2022b. Scaling Mean Field Games by Online Mirror Descent. In *Proceedings of the 21st International Conference on Autonomous Agents and Multiagent Systems*, AAMAS '22, 1028–1037. Richland, SC: International Foundation for Autonomous Agents and Multiagent Systems. ISBN 9781450392136.
- Perrin, S.; Laurière, M.; Pérolat, J.; Elie, R.; Geist, M.; and Pietquin, O. 2022. Generalization in mean field games by learning master policies. In *Proceedings of the AAAI Conference on Artificial Intelligence*, volume 36, 9413–9421.
- Perrin, S.; Laurière, M.; Pérolat, J.; Geist, M.; Elie, R.; and Pietquin, O. 2021. Mean Field Games Flock! The Reinforcement Learning Way. In *IJCAI*.
- Perrin, S.; Pérolat, J.; Laurière, M.; Geist, M.; Elie, R.; and Pietquin, O. 2020. Fictitious Play for Mean Field Games: Continuous Time Analysis and Applications. In *Proceedings of the 34th International Conference on Neural Information Processing Systems*, NIPS'20. Red Hook, NY, USA: Curran Associates Inc. ISBN 9781713829546.
- Saldi, N.; Başar, T.; and Raginsky, M. 2018. Markov–Nash Equilibria in Mean-Field Games with Discounted Cost. *SIAM Journal on Control and Optimization*, 56(6): 4256–4287.
- Subramanian, J.; and Mahajan, A. 2019. Reinforcement Learning in Stationary Mean-Field Games. In *Proceedings of the 18th International Conference on Autonomous Agents and MultiAgent Systems*, AAMAS '19, 251–259. Richland, SC: International Foundation for Autonomous Agents and Multiagent Systems. ISBN 9781450363099.
- Subramanian, S. G.; Poupart, P.; Taylor, M. E.; and Hegde, N. 2022. Multi Type Mean Field Reinforcement Learning. arXiv:2002.02513.
- Subramanian, S. G.; Taylor, M. E.; Crowley, M.; and Poupart, P. 2020. Partially Observable Mean Field Reinforcement Learning.
- Subramanian, S. G.; Taylor, M. E.; Crowley, M.; and Poupart, P. 2021. Decentralized Mean Field Games.
- Toumi, N.; Malhame, R.; and Le Ny, J. 2024. A mean field game approach for a class of linear quadratic discrete choice problems with congestion avoidance. *Automatica*, 160: 111420.
- uz Zaman, M. A.; Koppel, A.; Bhatt, S.; and Başar, T. 2023. Oracle-free Reinforcement Learning in Mean-Field Games along a Single Sample Path. arXiv:2208.11639.
- Vieillard, N.; Pietquin, O.; and Geist, M. 2020. Munchausen Reinforcement Learning. In Laroche, H.; Ranzato, M.; Hadsell, R.; Balcan, M.; and Lin, H., eds., *Advances in Neural Information Processing Systems*, volume 33, 4235–4246. Curran Associates, Inc.
- Wu, Z.; Lauriere, M.; Chua, S. J. C.; Geist, M.; Pietquin, O.; and Mehta, A. 2024. Population-aware Online Mirror Descent for Mean-Field Games by Deep Reinforcement Learning. arXiv:2403.03552.



Xie, Q.; Yang, Z.; Wang, Z.; and Minca, A. 2021. Learning While Playing in Mean-Field Games: Convergence and Optimality. In Meila, M.; and Zhang, T., eds., *Proceedings of the 38th International Conference on Machine Learning*, volume 139 of *Proceedings of Machine Learning Research*, 11436–11447. PMLR.

Yang, Y.; Luo, R.; Li, M.; Zhou, M.; Zhang, W.; and Wang, J. 2018. Mean Field Multi-Agent Reinforcement Learning. In Dy, J.; and Krause, A., eds., *Proceedings of the 35th International Conference on Machine Learning*, volume 80 of *Proceedings of Machine Learning Research*, 5571–5580. PMLR.

Yardim, B.; Cayci, S.; Geist, M.; and He, N. 2023. Policy Mirror Ascent for Efficient and Independent Learning in Mean Field Games. In *International Conference on Machine Learning*, 39722–39754. PMLR.

Yardim, B.; Goldman, A.; and He, N. 2024. When is Mean-Field Reinforcement Learning Tractable and Relevant? *arXiv preprint arXiv:2402.05757*.

Yongacoglu, B.; Arslan, G.; and Yüksel, S. 2022. Independent Learning in Mean-Field Games: Satisficing Paths and Convergence to Subjective Equilibria.

## Technical appendices to ‘Networked Communication for Mean-Field Games with Function Approximation and Empirical Mean-Field Estimation’

### A Experiments

For reproducibility, the code to run our experiments is provided with our Supplementary Materials, and will be made publicly available upon publication.

Experiments were conducted on a Linux-based machine with 2 x Intel Xeon Gold 6248 CPUs (40 physical cores, 80 threads total, 55 MiB L3 cache). We use the JAX framework to accelerate and vectorise our code. Random seeds are set in our code in a fixed way dependent on the trial number to allow easy replication of experiments - please see the code files in the Supplementary Materials for details.

#### A.1 Games

We conduct numerical tests with four games (defined by the agents’ reward/transition functions), chosen for being particularly amenable to intuitive and visualisable understanding of whether the agents are learning behaviours that are appropriate and explainable for the respective objective functions. In all cases, rewards are normalised in [0,1] after they are computed.

**Cluster.** This is the inverse of the ‘exploration’ game in (Lauriere et al. 2022), where in our case agents are encouraged to gather together by the reward function  $R(s_t^i, a_t^i, \hat{\mu}_t) = \log(\hat{\mu}_t(s_t^i))$ . That is, agent  $i$  receives a reward that is logarithmically proportional to the fraction of the population that is co-located with it at time  $t$ . We give the population no indication where they should cluster, agreeing this themselves over time.

**Agree on a single target.** Unlike in the above ‘cluster’ game, the agents are given options of locations at which to gather, and they must reach consensus among themselves. If the agents are co-located with one of a number of specified targets  $\phi \in \Phi$  (in our experiments we place one target in each of the four corners of the grid), and other agents are also at that target, they get a reward proportional to the fraction of the population found there; otherwise they receive a penalty of -1. In other words, the agents must coordinate on which of a number of mutually beneficial points will be their single gathering place. Define the magnitude of the distances between  $x, y$  at  $t$  as  $dist_t(x, y)$ . The reward function is given by  $R(s_t^i, a_t^i, \hat{\mu}_t) = r_{targ}(r_{collab}(\hat{\mu}_t(s_t^i)))$ , where

$$r_{targ}(x) = \begin{cases} x & \text{if } \exists \phi \in \Phi \text{ s.t. } dist_t(s_t^i, \phi) = 0 \\ -1 & \text{otherwise,} \end{cases}$$

$$r_{collab}(x) = \begin{cases} x & \text{if } \hat{\mu}_t(s_t^i) > 1/N \\ -1 & \text{otherwise.} \end{cases}$$

**Evade shark in shoal.** Define the magnitude of the horizontal and vertical distances between  $x, y$  at  $t$  as  $dist_t^h(x, y)$  and  $dist_t^v(x, y)$  respectively. The state  $s_t^i$  now consists of agent  $i$ ’s position  $x_t^i$  and the ‘shark’s’ position  $\phi_t$ . At each time step, the shark steps towards the most populated grid point  $x_t^* = \arg \max_{x \in \mathcal{S}} \hat{\mu}_t(x)$ . A horizontal step is taken

if  $dist_t^h(\phi_t, x_t^*) \geq dist_t^v(\phi_t, x_t^*)$ , otherwise a vertical step is taken. Additionally, the shark moves in a random direction with probability 0.01. Agents are rewarded more for being further from the shark, and also for clustering with other agents. The reward function is given by

$$R(s_t^i, a_t^i, \hat{\mu}_t) = dist_t^h(\phi_t, x_t^i) + dist_t^v(\phi_t, x_t^i) + \text{norm}_{dist}(\log(\hat{\mu}_t(x_t^i))),$$

where  $\text{norm}_{dist}(\cdot)$  indicates that the final term is normalised to have the same maximum and minimum values as the total combined vertical and horizontal distance.

**Push object to edge.** As before, define the magnitude of the horizontal and vertical distances between  $x, y$  at  $t$  as  $dist_t^h(x, y)$  and  $dist_t^v(x, y)$  respectively. The state  $s_t^i$  consists of agent  $i$ 's position  $x_t^i$  and the object's position  $\phi_t$ . The number of agents in the positions surrounding the object at time  $t$  generates a probability field around the object, such that the object is most likely to move in the direction away from the side with the most agents. As such, if agents are equally distributed around the object, it will be equally likely to move in any direction, but if they coordinate on choosing the same side, they can 'push' it in a certain direction. If  $\text{Edges} = \{\text{edge}^1, \dots, \text{edge}^4\}$  are the grid edges, the closest edge to the object at time  $t$  is given by  $\text{edge}_t^* = \arg \min_{\text{edge} \in \text{Edges}} (\min(dist_t^h(\phi_t, \text{edge}), dist_t^v(\phi_t, \text{edge})))$ . Agents are rewarded for how close they are to the object, and for how close the object is to the edge of the grid. The reward function is given by

$$R(s_t^i, a_t^i, \hat{\mu}_t) = dist_t^h(\phi_t, x_t^i) + dist_t^v(\phi_t, x_t^i) + dist_t^h(\phi_t, \text{edge}_t^*) + dist_t^v(\phi_t, \text{edge}_t^*).$$

**Diffuse.** We conduct an additional experiment not mentioned in the main text, which is similar to the 'exploration' tasks in Lauriere et al. (2022), Wu et al. (2024) and other MFG works. In our version agents are rewarded for being located in more sparsely populated areas but only if they are stationary. The reward function is given by  $R(s_t^i, a_t^i, \hat{\mu}_t) = r_{stationary}(-\hat{\mu}_t(s_t^i))$ , where

$$r_{stationary}(x) = \begin{cases} x & \text{if } a_t^i \text{ is 'remain stationary'} \\ -1 & \text{otherwise.} \end{cases}$$

## A.2 Experimental metrics

To give as informative results as possible about both performance and proximity to the MFNE, we provide two metrics for each experiment. Both metrics are plotted with mean and standard deviation, computed over the ten trials (each with a random seed) of the system evolution in each setting.

**Exploitability** Works on MFGs most commonly use the *exploitability* metric to evaluate how close a given policy  $\pi$  is to a NE policy  $\pi^*$  (Lauriere et al. 2022; Perrin et al. 2020; Laurière et al. 2022; Algumaei et al. 2023; Pérolat et al. 2022b; Benjamin and Abate 2024; Wu et al. 2024). The metric usually assumes that all agents are following the same policy  $\pi$ , and quantifies how much an agent can benefit by deviating from  $\pi$  by measuring the difference between the return given by  $\pi$  and that of a *BR* policy with respect to the distribution indicated by  $\pi$ :

**Definition 9 (Exploitability of  $\pi$ )** The exploitability  $Ex$  of policy  $\pi$  is given by:

$$Ex(\pi) = V(BR(I(\pi)), I(\pi)) - V(\pi, I(\pi)).$$

If  $\pi$  has a large exploitability then an agent can significantly improve its return by deviating from  $\pi$ , meaning that  $\pi$  is far from  $\pi^*$ , whereas an exploitability of 0 implies that  $\pi = \pi^*$ . Prior works conducting empirical testing have generally focused on the centralised setting, so this classical definition, as well as most evaluations, only consider exploitability when all agents are following a single policy  $\pi_k$ . However, Benjamin and Abate (2024) notes that purely independent agents, as well as networked agents, may have divergent policies  $\pi_k^i \neq \pi_k^j \forall i, k \in 1, \dots, N$ , as in our own setting. We therefore are interested in the 'exploitability' of the population's joint policy  $\pi := (\pi^1, \dots, \pi^N) \in \Pi^N$ .

Since we do not have access to the exact *BR* policy as in some related works (Lauriere et al. 2022; Wu et al. 2024), we must instead approximate the exploitability, similarly to (Perrin et al. 2021; Benjamin and Abate 2024). We freeze the policy of all agents apart from a deviating agent, for which we store its current policy and then conduct 50  $k$  loops of policy improvement. To approximate the expectations in Def. 9, we take the best return of the deviating agent across 10 additional  $k$  loops, as well as the mean of all the other agents' returns across these same 10 loops. (While the policies of all non-deviating agents is  $\pi_k$  in the centralised case, if the non-deviating agents do not share a single policy, then this method is in fact approximating the exploitability of their joint policy  $\pi_k^{-d}$ , where  $d$  is the deviating agent.) We then revert the agent back to its stored policy, before learning continues for all agents as per the main algorithm. Due to the expensive computations required for this metric, we evaluate it every second  $k$  iteration of the main algorithm for Figs. 1, 2, 7, 8 and 9, and every fourth iteration for the population-dependent experiments.

The exploitability metric has a number of limitations in our setting. Our approximation takes place via MOMD policy improvement steps (as in the main algorithm) for a independent, deviating agent while the policies of the rest of the population are frozen. As such, the quality of our approximation is limited by the number of policy improvement/expectation rounds, which must be restricted for the sake of running speed of the experiments. Moreover, since one of the findings of our paper is that networked agents can improve their policies faster than independent or centralised agents, especially when non-linear function approximation is used, it is arguably unsurprising that approximating the *BR* by an independently deviating agent sometimes gives an unclear and noisy metric. This includes the exploitability going below zero, which should not be possible if the policies and distributions are computed exactly.

Moreover, in coordination games (the setting on which we focus), agents benefit by following the same behaviour as others, and so a deviating agent generally stands to gain less from a *BR* policy than it might in the non-coordination games on which many other works focus. For example, the return of a best-responding agent in the 'push object' game still depends on the extent to which other agents coordinate

on which direction in which to push the box, meaning it cannot significantly increase its return by deviating. This means that the downward trajectory of the exploitability metric is less clear in our plots than in other works. This is likely why the approximated exploitability gets lower in the ‘disperse’ task in Fig. 8 than in the other tasks. Given the limitations presented by approximating exploitability, we also provide the second metric to indicate the progress of learning.

**Average discounted return** We record the average discounted return of the agents’ policies  $\pi_k^i$  during the  $M$  iterations - this allows us to observe that settings that converge to similar exploitability values may not have similar average agent returns, suggesting that some algorithms are better than others at finding not just NE, but preferable NE. See for example Figs. 1 and 7, where the networked agents converge to similar exploitability as the independent and centralised agents, but receive higher average returns.

### A.3 Hyperparameters

See Table 1 for our hyperparameter choices. We can group our hyperparameters into those controlling the size of the experiment, those controlling the size of the Q-network, those controlling the number of iterations of each loop in the algorithms and those affecting the learning/policy updates or policy adoption.

In our experiments we generally want to demonstrate that our communication-based algorithms outperform the centralised and independent architectures by allowing policies that are estimated to be better performing to proliferate through the population, such that convergence occurs within fewer iterations and computationally faster, even when the Q-function is poorly approximated and/or the mean-field is poorly estimated, as is likely to be the case in real-world scenarios. Moreover we want to show that there is a benefit even to a small amount of communication, so that communication rounds themselves do not excessively add to time complexity. As such, we generally select hyperparameters at the lowest end of those we tested during development, to show that our algorithms are particularly successful given what might otherwise be considered ‘undesirable’ hyperparameter choices.

### A.4 Additional experiments

We provide additional experiments on large grids in Figs. 7, 8 and 9. In the ‘target agreement’ task in Fig. 7, the networked agents all significantly outperform both centralised and independent agents in term of average return, despite the independent agents appearing to have slightly lower exploitability. This is because independent agents are hardly improving their policies at all, such that there is little a deviating agent can do to increase its return in this coordination game, such that exploitability appears low, despite this being an undesirable equilibrium (see Appx. A.2 for further discussion on the limited information provided by the exploitation metric). In the ‘cluster’ task in Fig. 9, the networked agents obtain significantly higher return than the independent agents. While centralised agents have the lowest exploitability, networked agents of almost all communication

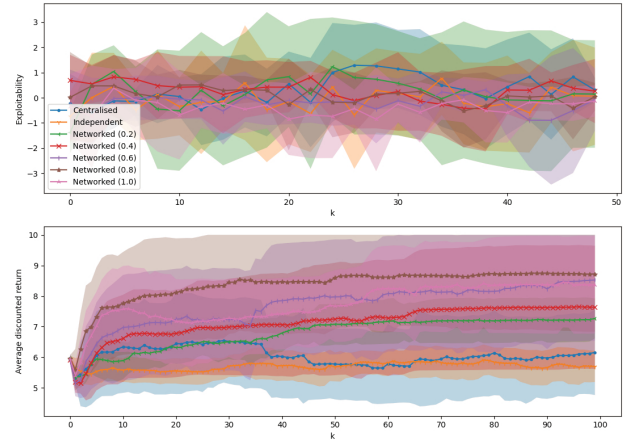


Figure 5: ‘Push object’ task, population-dependent policies with global observability of mean-field distribution, 10x10 grid.

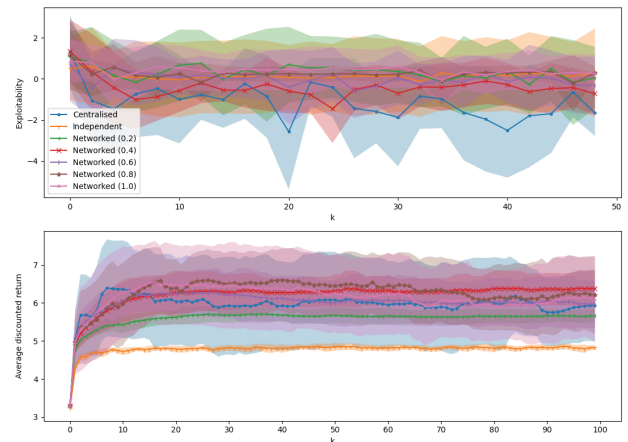


Figure 6: ‘Evade’ task, population-dependent policies with global observability of mean-field distribution, 10x10 grid.

radii outperform them in terms of average return, indicating that the communication scheme helps populations reach better performing equilibria.

In the additional ‘disperse’ task in Fig. 8, networked agents significantly outperform independent and centralised agents in terms of average return. They also outperform centralised agents in terms of exploitability, and significantly outperform independent agents in terms of exploitability.

### Explanation of better performance by networked agents than centralised agents

By adopting policy parameters  $\pi_{k+1}^j$  from neighbours with probability related to their estimated value  $\sigma_{k+1}^j$ , networked agents can adopt parameters that are estimated to be better performing than their own, which intuitively means networked agents improve their return quicker than agents learning entirely independently. Moreover, since the centralised case involves a single central agent training its Q-network and then pushing its update au-

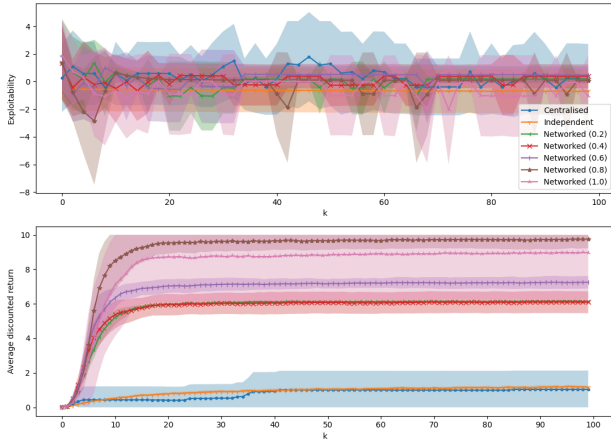


Figure 7: ‘Target agreement’ task, population-independent policies, 100x100 grid.

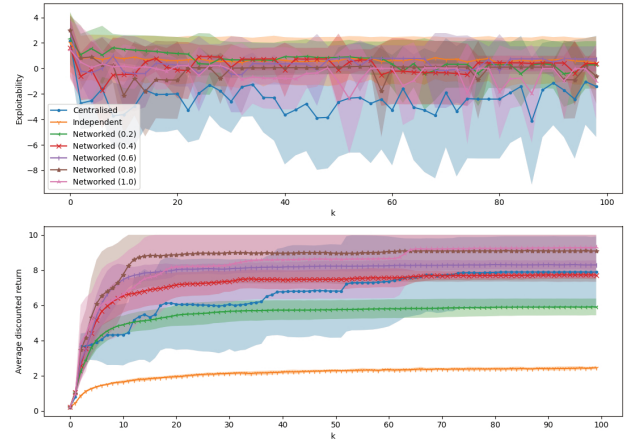


Figure 9: ‘Cluster’ task, population-independent policies, 50x50 grid.

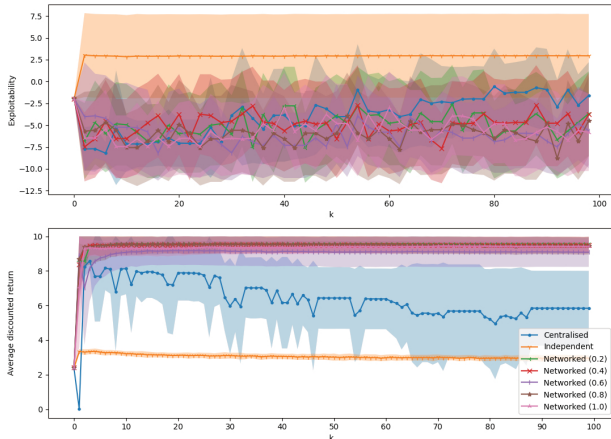


Figure 8: ‘Disperse’ task, population-independent policies, 100x100 grid.

tomatically to all the others, this single set of updated parameters will be taken on by all agents whether or not they are actually particularly well performing. Since the networked agents are more likely to select better performing parameters out of a variety of options according to our algorithm, we find networked agents usually in fact learn *quicker* than centralised agents, and indeed the benefit is even greater in the function approximation setting than in the tabular case given in Benjamin and Abate (2024). It is significant that our communication scheme not only allows us to avoid the undesirable assumption of a centralised learner, but even to outperform it.

## B Related work

MFGs are a quickly growing research area, so we only discuss the works most closely related to this present work, and instead refer the reader to Benjamin and Abate (2024) for detailed discussion around the setting of networked communication for MFGs, and to Laurière et al. (2022) for a

broader survey of MFGs. Our work is most closely related to Benjamin and Abate (2024), which introduced networked communication to the infinite-horizon MFG setting. However, this work focuses only on tabular settings rather than using function approximation as in ours, and only addresses population-independent policies.

Laurière et al. (2022) uses Munchausen Online Mirror Descent (MOMD), similar to our method for learning with neural networks, but there are numerous differences to our setting: most relevantly, they study a finite-horizon episodic setting, where the mean-field distribution is updated in an exact way and an oracle supplies a centralised learner with rewards and transitions for it to learn a population-independent policy. Wu et al. (2024) uses MOMD to learn population-dependent policies, albeit also with a centralised method that exactly updates the mean-field distribution in a finite-horizon episodic setting. Perrin et al. (2022) learns population-dependent policies with function approximation in infinite-horizon settings like our own, but does so in a centralised, two-timescale manner without using the empirical mean-field distribution.

Yongacoglu, Arslan, and Yüksel (2022) addresses decentralised learning from a continuous, non-episodic run of the empirical system using either full or compressed information about the mean-field distribution, but agents are assumed to receive this information directly, rather than estimating it locally as in the algorithm we now present. They also do not consider function approximation or inter-agent communication in their algorithms. In the closely related but distinct area of Mean-Field RL, Subramanian et al. (2020) does estimate the empirical mean-field distribution from the local neighbourhood, however agents are seeking to estimate the mean action rather than the mean-field distribution over states as in our MFG setting. Their agents also do not have access to a communication network by which they can improve their estimates.

## C Extensions and future work

Alg. 3, described in Sec. 4 assumes that if a state  $s'$  is connected to  $s$  on the visibility graph  $\mathcal{G}_t^{vis}$ , an agent in  $s$  is able to *accurately* count all the agents in  $s'$ , i.e. it either counts the exact total or cannot observe the state at all. While we assume this for simplicity, this is not inherently the case, since a real-world agent may have only noisy observations even of others located nearby, due to imperfect sensors. We suggest two ways to deal with this case. Firstly, if agents share unique IDs as in Alg. 2, then when communicating their vectors of collected IDs with each other via  $\mathcal{G}_t^{comm}$ , agents would gain the most accurate picture possible of all the agents that have been observed in a given state. However, as we note in the main body of the paper, there are various reasons why sharing IDs might be undesirable, including privacy and scalability. If instead only counts are taken, and if the noise on each agents' count is assumed to be independent and, for example, subject to a Gaussian distribution, the algorithm can easily be updated such that communicating agents compute averages of their local and received counts to improve their accuracy, rather than simply using communication to fill in counts for previously unobserved states. (Note that we can also consider the original case without noise to involve averaging, since averaging identical values equates to using the original value). Since the algorithm is intended to aid in local estimation of the mean-field distribution, which is inherently approximate due to the uniform method for distributing the uncounted agents, we are not concerned with reaching exact consensus between agents on the communicated counts, such that we do not require repeated averaging to ensure asymptotic convergence.

We may also wish to consider more sophisticated methods for distributing the uncounted agents across states, in place of the uniform distribution we use now. Such choices may be domain-specific based on knowledge of a particular environment. For example, one might in fact use the counts to perform Bayesian updates on a specific prior, where this prior may relate to the estimated mean-field distribution at the previous time step  $t - 1$ . If agents seek to learn to predict the *evolution* of the mean field based on their own policy or by learning a model, the Bayesian prior may also be based on forward prediction from the estimated mean-field distribution at  $t - 1$ . Future work lies in conducting experiments in all of these more general settings.

Perrin et al. (2022) notes that in grid-world settings such as those in our experiments, passing the (estimated or true global) mean-field distribution as a flat vector to the Q-network ignores the geometric structure of the problem. They therefore propose to create an embedding of the distribution by first passing the vector to a convolutional neural network, essentially treating the categorical distribution as an image. This technique is also followed in (Wu et al. 2024) (for their additional experiments, but not in the main body of their paper). As future work, we can test whether such a method improves the performance of our algorithms.

As in the closely-related work by Wu et al. (2024), we conduct extensive numerical experiments to demonstrate the benefits of our algorithm over baselines, and leave the theoretical analysis, such proof of convergence in the function

approximation setting, for future work.

## D Additional remarks

In our Algs. 2 and 3, agents share their local *counts* with neighbours on the communication network  $\mathcal{G}_t^{comm}$ , and only after the  $C_e$  communication rounds do they complete their estimated distribution by distributing the uncounted agents along their vectors. An alternative would be for each agent to immediately form a local *estimate* from their local count obtained via  $\mathcal{G}_t^{obs}$  or  $\mathcal{G}_t^{vis}$ , which is only then communicated and updated via the communication network. However, we take the former approach to avoid poor local estimations spreading through the network and leading to widespread inaccuracies. Information that is certain (the count) is spread as widely as possible, before being locally converted into an estimate of the total mean field. The same would be the case in our proposed extension for averaging noisy counts i.e. only the counts would be averaged, with the estimates completed by distributing the remaining agents after the  $C_e$  communication rounds.

Hyperparam.	Value	Comment
Trials	10	We run 10 trials with different random seeds for each experiment. We plot the mean and standard deviation for each metric across the trials.
Gridsize	10x10 / 50x50 / 100x100	Experiments with population-dependent policies are run on the 10x10 grid (Figs. 3, 4, 5 and 6), while experiments on large state spaces are run on 50x50 and 100x100 grids (Figs. 1, 2, 7, 8 and 9).
Population	500	We chose 500 for our demonstrations to show that our algorithm can handle large populations, indeed often larger than those demonstrated in other mean-field works, especially for grid-world environments, while also being feasible to simulate wrt. time and computation constraints (Yongacoglu, Arslan, and Yüksel 2022; Cui and Koepl 2021; Cui, Fabian, and Koepl 2023; Guo et al. 2020; Subramanian and Mahajan 2019; Yang et al. 2018; Subramanian et al. 2020, 2022, 2021; Wu et al. 2024; Benjamin and Abate 2024).
Number of neurons in input layer	cf. comment	The agent’s position is represented by two concatenated one-hot vectors indicating the agent’s row and column. An additional two such vectors are added for the shark’s/object’s position in the ‘evade’ and ‘push object’ tasks. For population-dependent policies, the mean-field distribution is a flattened vector of the same size as the grid. As such, the input size in the ‘evade’ and ‘push object’ tasks is $[(4 \times \text{dimension}) + (\text{dimension}^2)]$ ; in the other settings it is $[2 \times \text{dimension}]$ .
Neurons per hidden layer	cf. comment	We draw inspiration from common rules of thumb when selecting the number of neurons in hidden layers, e.g. it should be between the number of input neurons and output neurons / it should be 2/3 the size of the input layer plus the size of the output layer / it should be a power of 2 for computational efficiency. Using these rules of thumb as rough heuristics, we select the number of neurons per hidden layer by rounding the size of the input layer down to the nearest power of 2. The layers are all fully connected.
Hidden layers	2	We experimented with 2 and 3 hidden layers in the Q-networks. While 3 hidden layers gave similar or slightly better performance, we selected 2 for increased computational speed for conducting our experiments.
Activation function	ReLU	This is a common choice in deep RL.
$K$	100	$K$ is chosen to be large enough to see at least one of the metrics converging.
$M$	50	We tested $M$ in $\{50,100\}$ and found that the lower value was sufficient to achieve convergence while minimising training time. It may be possible to converge with even smaller choices of $M$ .
$L$	50	We tested $L$ in $\{50,100\}$ and found that the lower value was sufficient to achieve convergence while minimising training time. It may be possible to converge with even smaller choices of $L$ .
$E$	20	We tested $E$ in $\{20,50,100\}$ , and choose the lowest value to show the benefit to convergence even from very few evaluation steps. It may be possible to reduce this value further and still achieve similar results.
$C_p$	1	As in Benjamin and Abate (2024), we choose this value to show the convergence benefits brought by even a single communication round, even in networks that may have limited connectivity; higher choices are likely to have even better performance.
$C_e$	1	Similar to $C_p$ , we choose this value to show the ability of our algorithm to appropriately estimate the mean field even with only a single communication round, even in networks that may have limited connectivity.
$\gamma$	0.9	Standard choice across RL literature.
$\tau_q$	0.03	We tested $\tau_q$ in $\{0.01,0.02,0.03,0.04,0.05\}$ , as well as linearly decreasing $\tau_q$ from $0.05 \rightarrow 0$ as $k$ increases. However, only 0.03 gave stable increase in return. Note that this is the value also chosen in Vieillard, Pietquin, and Geist (2020).
$ B $	32	This is a common choice of batch size that trades off noisy updates and computational efficiency.
$cl$	-1	We use the same value as in Vieillard, Pietquin, and Geist (2020).
$\nu$	$L - 1$	We tested $\nu$ in $\{1, 4, 20, L - 1\}$ . We found that in our setting, updating $\theta' \leftarrow \theta$ once per $k$ iteration s.t. $\theta'_{k+1,l} = \theta_{k,l} \forall l$ gave sufficient learning that was similar to the other potential choices of $\nu$ , so we do this for simplicity, rather than arbitrarily choosing a frequency to update $\theta'$ during each $k$ loop. Setting the target to be the policy from the previous iteration is similar to the method in Lauriere et al. (2022). Whilst Wu et al. (2024) updates the target within the $L$ loops for stability, we do not find this to be a problem in our experiments.
Optimiser	Adam	As in Vieillard, Pietquin, and Geist (2020), we use the Adam optimiser with initial learning rate 0.01.
$\tau_k$	cf. comment	$\tau_k$ increases linearly from 0.001 to 1 across the $K$ iterations. This is a simplification of the annealing scheme used in Benjamin and Abate (2024). Further optimising the annealing process may lead to better results.

Table 1: Hyperparameters